Supplementary information (SI) for

Tunable magnetism in two-dimensional ferroelectric Janus NbOXY (X, Y = Cl, Br, I; X ≠ Y) by hole-doping

Yunlai Zhu [a], Xi Sun [a], Yongjie Zhao [a], Junjie Zhang [a], Ying Zhu [a], Tong Zhu [a], Ke Wang [a], Zuyu Xu [a], Zuheng Wu [a]*, and Yuehua Dai [a]*

[a] School of Integrated Circuits, Anhui University, Hefei, Anhui, 230601, China.

Corresponding Authors

*E-mail: wuzuheng@ahu.edu.cn (Z.-H. Wu), daiyuehua2013@163.com (Y.-H. Dai)

Table S1 Lattice constants *a*, *b* and *c*(Å), bond length Nb-O and atomic spacing Nb-Nb(Å), bond angles ∠X-Nb-X, ∠Y-Nb-Y and ∠X-Nb-Y (°) of NbOXY monolayer.

Crystal	NbOClBr	NbOClI	NbOBrI
a	3.922	3.925	3.929
b	6.942	7.244	7.383
c	3.898	3.908	4.212
Nb-O1	1.809	1.821	1.823
Nb-O2	2.115	2.106	2.107
Nb-Nb1	3.981	4.280	4.339
Nb-Nb2	2.961	2.964	3.044
∠X-Nb-X	105.22	105.35	108.02
∠Y-Nb-Y	83.96	84.28	82.69
∠X-Nb-Y	84.84	84.73	84.26

Table S2 The total magnetic moment μ_{Total} (μ_B), average magnetic moment μ (μ_B/hole), ferromagnetic energy E_{FM} (eV), non-magnetic energy E_{NM} (eV), spin polarization energy E_{SP} (meV/hole), and spontaneous polarization intensity P_s (10^{-10}C/m) of NbOClBr supercell under different hole doping concentrations.

ρ	μ_{Total}	μ	E_{NM}	E_{FM}	E_{SP}	P_s
0	0.00	0.00	-102.233	-102.233	0.000	1.959
0.1	0.40	1.00	-100.573	-100.583	24.398	1.845
0.2	0.80	1.00	-98.448	-98.471	28.482	1.925
0.3	1.08	0.90	-95.858	-95.937	65.945	2.003
0.4	1.14	0.71	-92.659	-92.843	115.397	2.069
0.5	1.99	0.99	-88.950	-89.193	121.665	2.190
0.6	1.23	0.52	-84.854	-84.959	43.598	2.219
0.7	0.80	0.29	-80.109	-80.137	9.876	2.321
0.8	0.51	0.16	-74.789	-74.790	0.486	2.314

Table S3 The total magnetic moment (μ_B) of NbOClBr monolayer doped with 0.5 u.c.$^{-1}$ holes under different strains on the x-axis and y-axis.

strain(%)	μ_{Total}(*x*-axis)	μ_{Total}(*y*-axis)
-5	0.00	0.00
-4	0.00	0.00
-3	0.00	0.00
-2	0.00	0.00
-1	0.00	0.00
+1	1.94	2.00
+2	1.96	2.00
+3	1.98	2.00
+4	1.99	2.00
+5	1.99	2.00

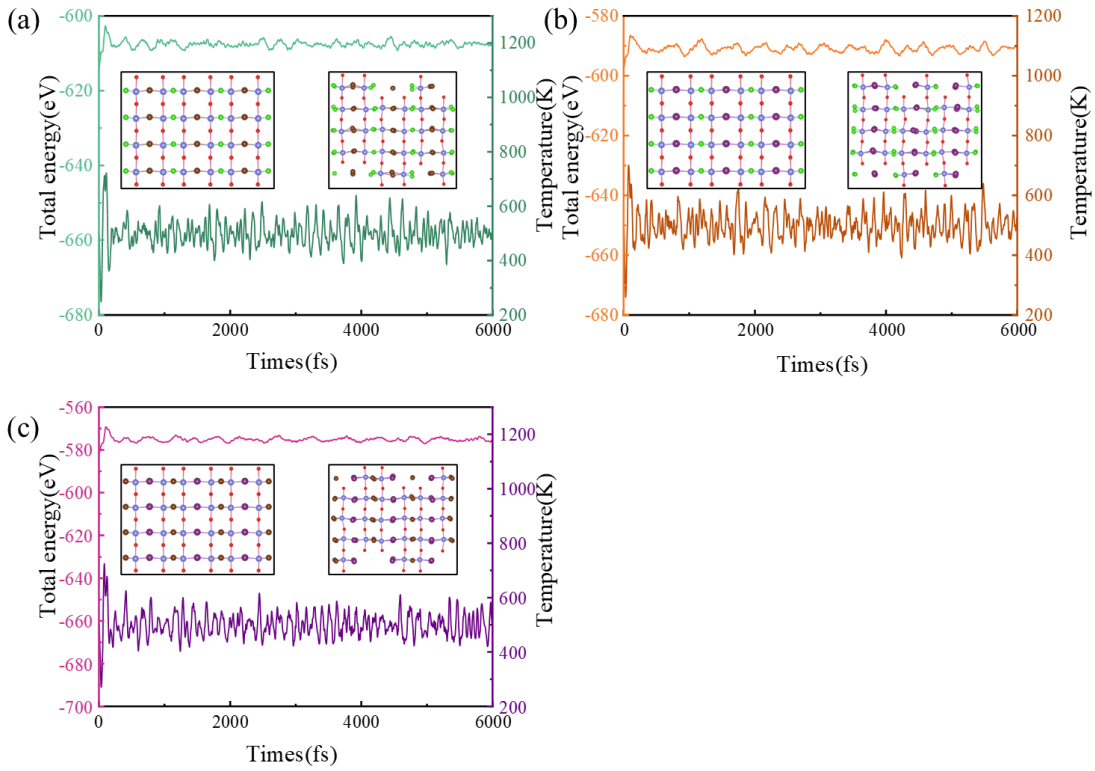

FIG. S1 The variation of total energy and the temperature during AIMD process at 300 K for a time step of 3 fs for (a) NbOClBr, (b) NbOClI and (c) NbOBrI. Inset shows the corresponding snapshots at the end of 6000 fs, indicating stable structure without phase change.

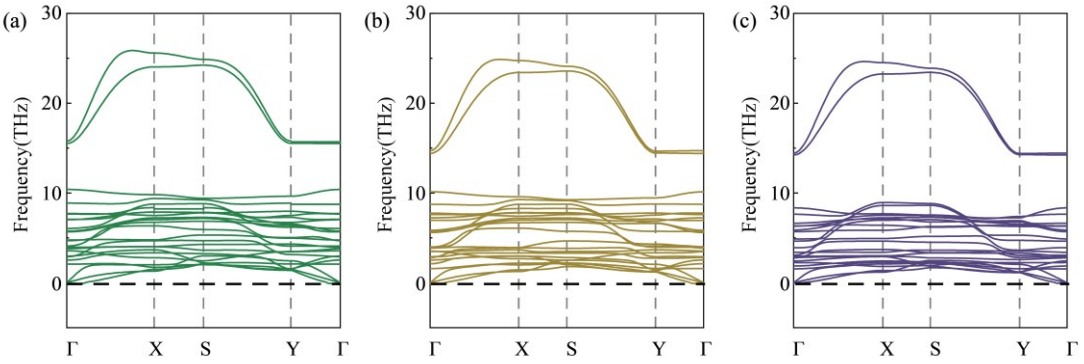

FIG. S2 Phonon dispersion curves for (a) NbOClBr, (b) NbOClI and (c) NbOBrI.

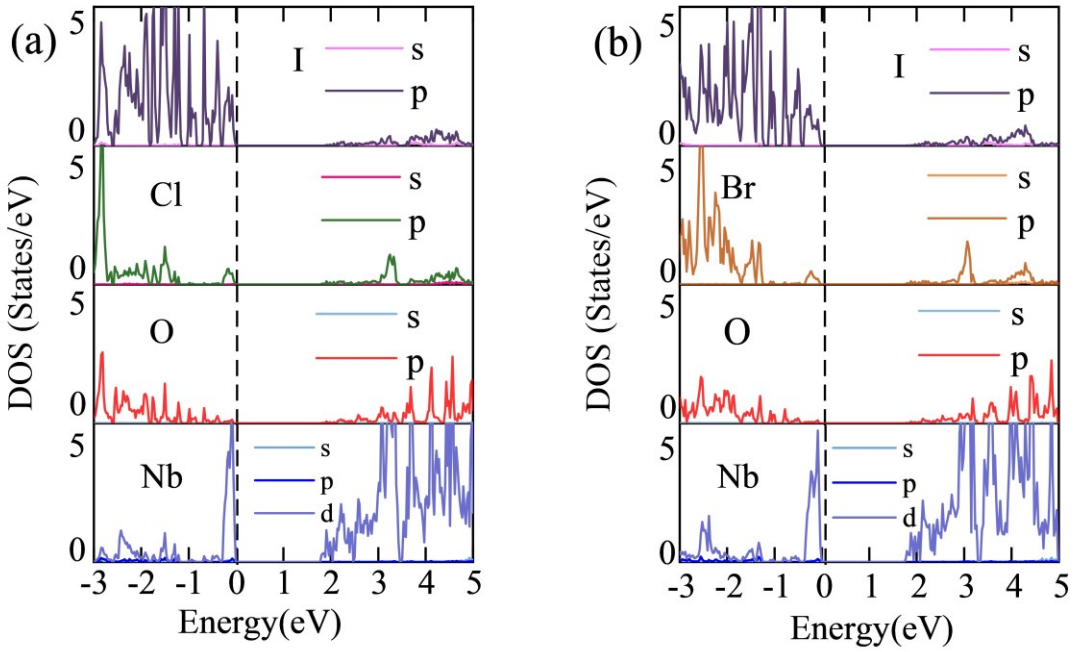

FIG. S3 Projected density of states for (a) NbOClI and (b) NbOBrI. The Fermi level is set to 0 eV.

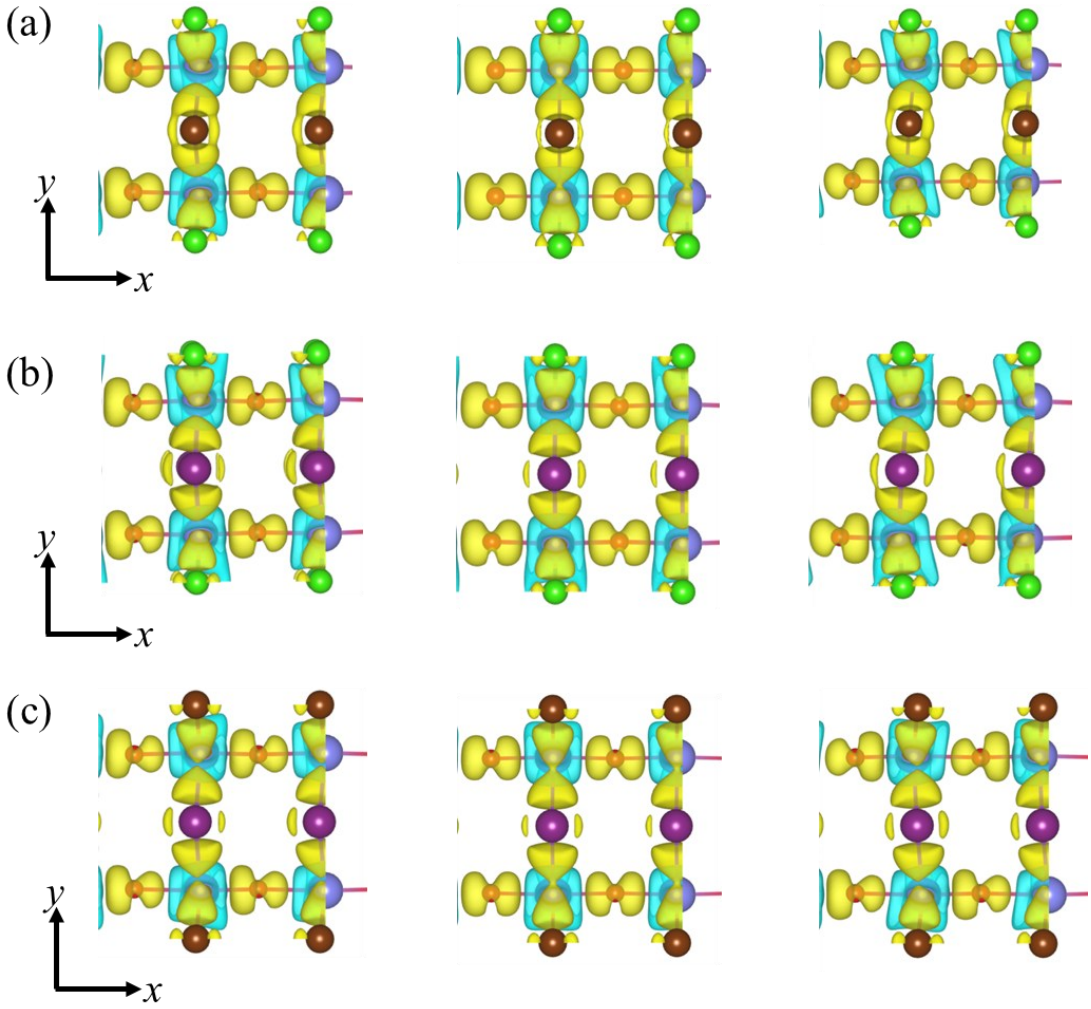

FIG. S4 Differential charge density for (a) NbOClBr, (b) NbOClI, and (c) NbOBrI in different polarity states (FE, PE, AFE states from left to right). The accumulation (depletion) of electrons is represented by yellow (blue).

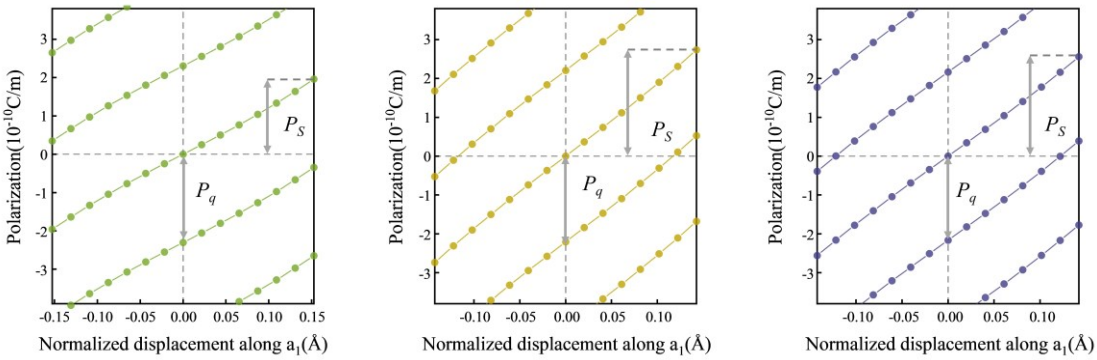

FIG. S5 Polarization curves of (a) NbOClBr, (b) NbOClI and (c) NbOBrI, where the polarization quantum P_q and spontaneous polarization P_s are marked.

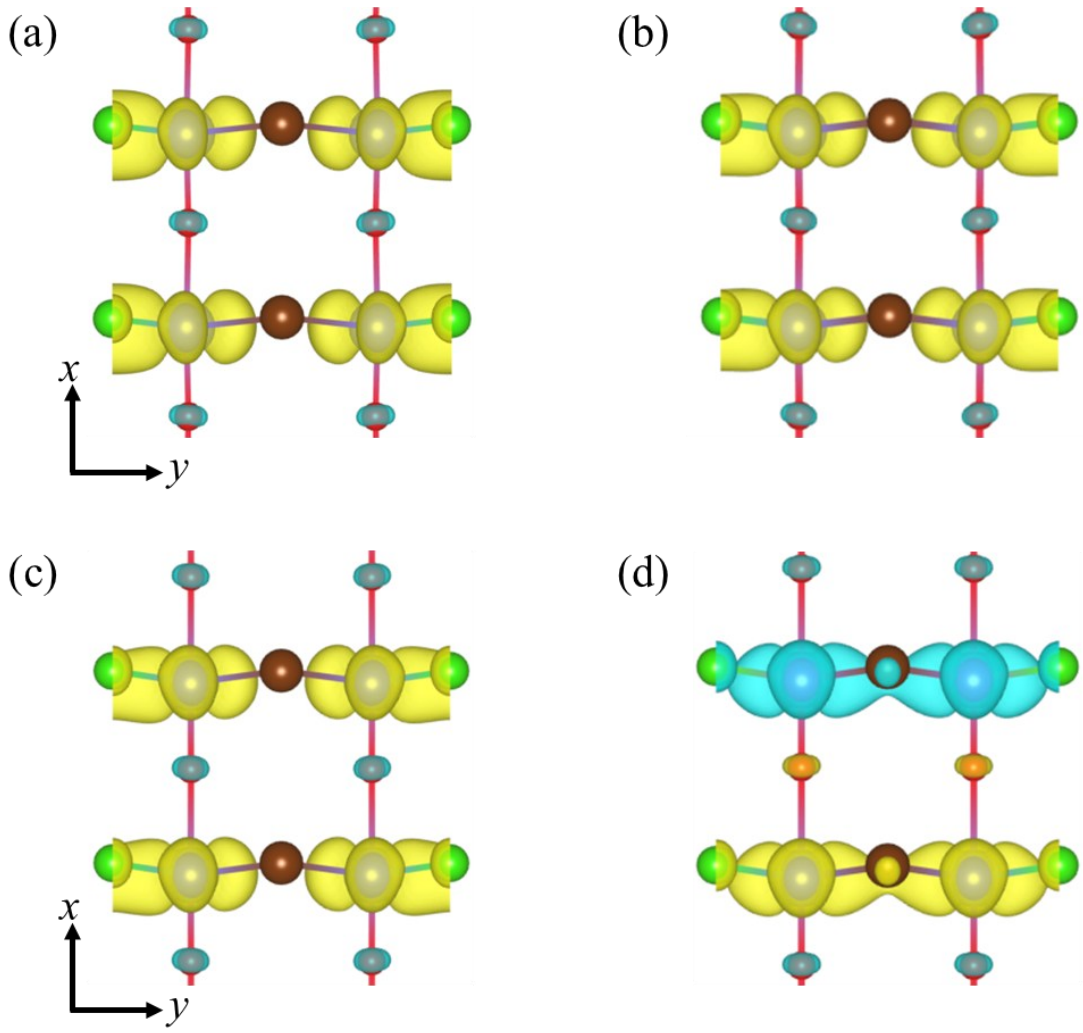

FIG. S6 Spin density distribution of NbOClBr monolayer at hole doping concentrations of (a) 0.1 u.c.$^{-1}$, (b) 0.3 u.c.$^{-1}$, (c) 0.5 u.c.$^{-1}$ and (d) 0.7 u.c.$^{-1}$. Yellow and cyan iso-surfaces represent the positive and negative spin densities, respectively. The iso-surfaces are 0.001 e/Å^3.

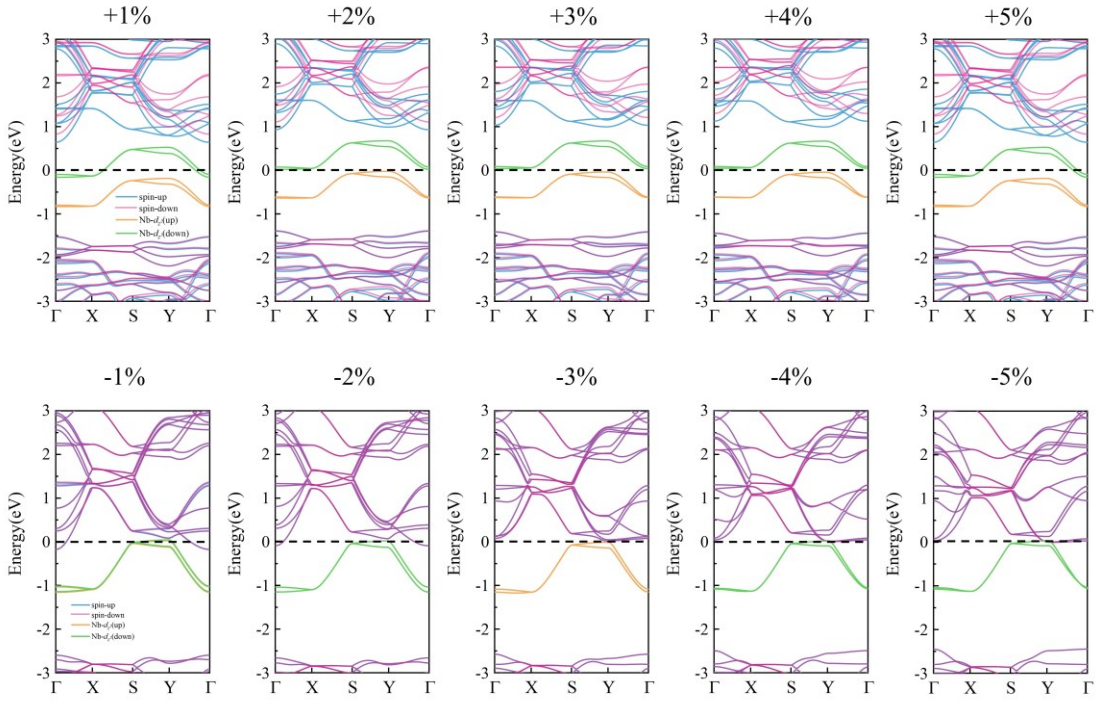

FIG. S7 Energy bands of NbOClBr monolayer doped with 0.5 u.c.$^{-1}$ holes under *x*-axis strain calculated using PBE methods.

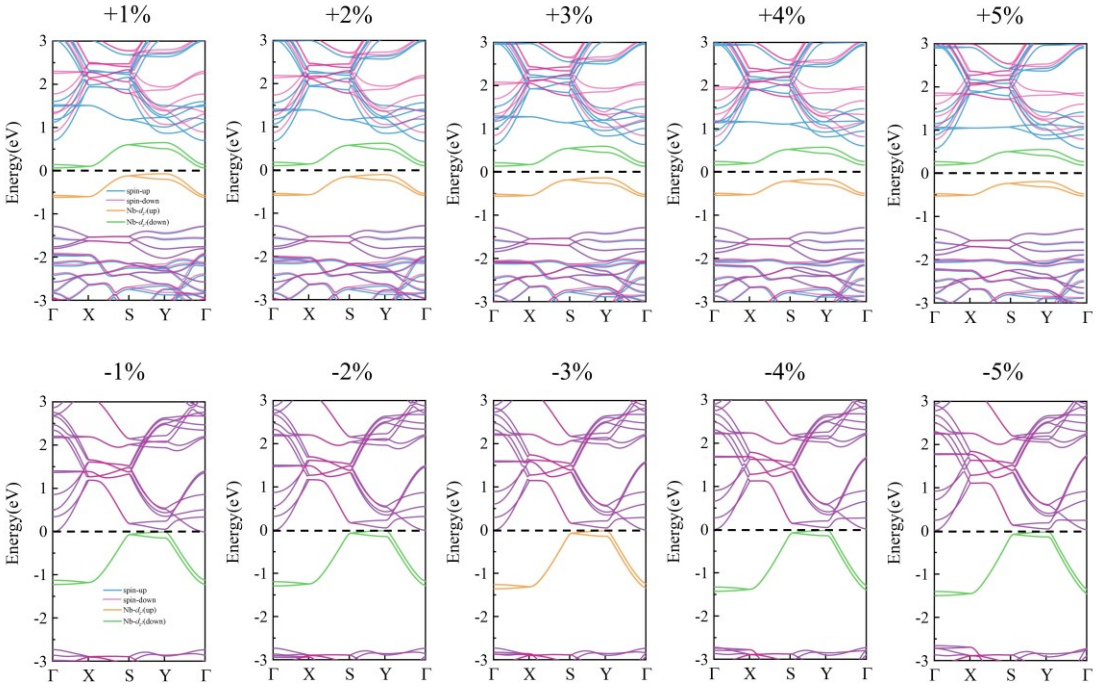

FIG. S8 Energy bands of NbOClBr monolayer doped with 0.5 u.c.$^{-1}$ holes under *y*-axis strain calculated using PBE methods.

Structural data for NbOXY monolayer:

FE phase in NbOClBr:

NbOClBr

1.00000000000000

3.9220982617078350	0.0000000000000000	0.0000000000000000
0.0000000000000000	6.9416973272758851	0.0000000000000000
0.0000000000000000	0.0000000000000000	24.2084999084000003

Nb	Cl	O	Br
2	2	2	2

Direct

0.9967179435970195	0.2132814660101303	0.4999996884448947
0.9967179435970195	0.7867185339898697	0.5000003115551053
0.9543844484170307	0.0000023658827430	0.5805164770150597
0.9543844484170307	0.9999977061172558	0.4194834449849409
0.4577712871969339	0.2211089021030048	0.4999986185305332
0.4577712871969339	0.7788911488969958	0.5000015004694660
0.9462864137890179	0.5000017108505048	0.4256629614448642
0.9462864137890179	0.4999983911494965	0.5743371565551314

AFE phase in NbOClBr:

NbOClBr

1.00000000000000

3.9220981598000000	0.0000000000000000	0.0000000000000000
0.0000000000000000	6.9416971206999998	0.0000000000000000
0.0000000000000000	0.0000000000000000	24.2084999084000003

Nb	Cl	O	Br
2	2	2	2

Direct

0.9188200239999986	0.2132814679999981	0.4999997019999967
0.9967179300000026	0.7867185469999995	0.5000002980000033
0.9543844459999988	0.0000023659999968	0.5805164579999982
0.9543844459999988	0.9999977350000009	0.4194834529999980
0.4577713010000011	0.2211088990000007	0.4999986289999967
0.4577713010000011	0.7788911459999994	0.5000014900000025
0.9462864400000015	0.5000017289999974	0.4256629650000008
0.9462864400000015	0.4999983909999983	0.5743371840000009

PE phase in NbOClBr:

NbOClBr

1.00000000000000

3.9220981598000000	0.0000000000000000	0.0000000000000000
0.0000000000000000	6.9416971206999998	0.0000000000000000
0.0000000000000000	0.0000000000000000	24.2084999084000003

Nb Cl O Br

2 2 2 2

Direct

0.9577699900000027 0.2211090030000022 0.4999997019999967

0.9577699900000027 0.7788910270000002 0.5000002980000033

0.9577699900000027 0.0000023659999968 0.5805164579999982

0.9577699900000027 0.9999977350000009 0.4194834529999980

0.4577713010000011 0.2211088990000007 0.4999986289999967

0.4577713010000011 0.7788911459999994 0.5000014900000025

0.9577699900000027 0.5000017289999974 0.4256629650000008

0.9577699900000027 0.4999983909999983 0.574337184000000

FE phase in NbOClI:

NbOClI

1.00000000000000

3.9254136377449820 0.0000000000000000 0.0000000000000000

0.0000000000000000 7.2441127843007749 0.0000000000000000

0.0000000000000000 0.0000000000000000 24.2084999084000003

Nb O I Cl

2 2 2 2

Direct

0.9940969284959422 0.2045691271266463 0.4999994191609858

0.9940969284959422 0.7954308728733537 0.5000000151609854

0.4577348740654301 0.2126003912021091 0.4999997205267945

0.4577348740654301 0.7873996387978934 0.5000025815267932

0.9488463300085215 0.5000017289999974 0.4197347004056908

0.9487568410560954 0.4999983909999983 0.5802663018404246

0.9545254819317179 0.9999977350000009 0.4192777538005643

0.9545279768809252 0.0000023659999968 0.5807196275777571

AFE phase in NbOClI:

NbOClI

1.00000000000000

3.9254136086000000 0.0000000000000000 0.0000000000000000

0.0000000000000000 7.2441129683999996 0.0000000000000000

0.0000000000000000 0.0000000000000000 24.2084999084000003

Nb O I Cl

2 2 2 2

Direct

0.9213630615040602 0.2045691309999995 0.4999994340000029

0.9577299950000011 0.7954308990000030 0.5000000000000000

0.4577348830000005 0.2126003950000026 0.4999997319999991

0.4577348830000005 0.7873996499999976 0.5000025630000025

0.9488463400000029 0.5000017289999974 0.4197346870000018

0.9487568139999993 0.4999983909999983 0.5802662970000014
0.9545254709999966 0.9999977350000009 0.4192777570000032
0.9545279740000012 0.0000023659999968 0.5807196499999989

PE phase in NbOClI:

NbOClI
1.00000000000000
3.9254136086000000 0.0000000000000000 0.0000000000000000
0.0000000000000000 7.2441129683999996 0.0000000000000000
0.0000000000000000 0.0000000000000000 24.2084999084000003
Nb O I Cl
2 2 2 2
Direct
0.9577299950000011 0.2045691309999995 0.4999994340000029
0.9577299950000011 0.7954308990000030 0.5000000000000000
0.4577348830000005 0.2126003950000026 0.4999997319999991
0.4577348830000005 0.7873996499999976 0.5000025630000025
0.9488463400000029 0.5000017289999974 0.4197346870000018
0.9487568139999993 0.4999983909999983 0.5802662970000014
0.9545254709999966 0.9999977350000009 0.4192777570000032
0.9545279740000012 0.0000023659999968 0.5807196499999989

FE phase in NbOBrI:

NbOBrI
1.00000000000000
3.9290389881230885 0.0000000000000000 0.0000000000000000
0.0000000000000000 7.3827771862123113 0.0000000000000000
0.0000000000000000 0.0000000000000000 24.2084999084000003
Nb O Br I
2 2 2 2
Direct
0.9938757033300050 0.2061374712539461 0.5000005089489505
0.9938757033300050 0.7938625737460541 0.5000011049489501
0.4576867005947420 0.2123729252989150 0.4999988444142929
0.4576867005947420 0.7876271347010828 0.5000017054142987
0.9544812361736632 0.0000023659999968 0.5869981146756871
0.9544462880518054 0.9999977350000009 0.4130015245910883
0.9491155616483482 0.4999983909999983 0.5791169594603787
0.9491522802766852 0.5000017289999974 0.4208813565463529

AFE phase in NbOBrI:

NbOBrI
1.00000000000000
3.9290390015000001 0.0000000000000000 0.0000000000000000

0.0000000000000000 7.3827772140999999 0.0000000000000000

0.0000000000000000 0.0000000000000000 24.2084999084000003

Nb O Br I

2 2 2 2

Direct

0.9938687089999974 0.2061319800000021 0.4999997319999991

0.9215210079999991 0.7938680649999981 0.5000003580000012

0.4576941130000023 0.2123623339999980 0.4999985099999975

0.4576941130000023 0.7876377110000021 0.5000013710000033

0.9544557330000032 0.0000023659999968 0.5869972110000035

0.9544513820000020 0.9999977350000009 0.4130029080000028

0.9491414430000020 0.4999983909999983 0.5791131260000029

0.9491459730000003 0.5000017289999974 0.4208868739999971

PE phase in NbOBrI:

NbOBrI

1.00000000000000

3.9290390015000001 0.0000000000000000 0.0000000000000000

0.0000000000000000 7.3827772140999999 0.0000000000000000

0.0000000000000000 0.0000000000000000 24.2084999084000003

Nb O Br I

2 2 2 2

Direct

0.9576900010000031 0.2061319800000021 0.4999997319999991

0.9576900010000031 0.7938680649999981 0.5000003580000012

0.4576941130000023 0.2123623339999980 0.4999985099999975

0.4576941130000023 0.7876377110000021 0.5000013710000033

0.9544557330000032 0.0000023659999968 0.5869972110000035

0.9544513820000020 0.9999977350000009 0.4130029080000028

0.9491414430000020 0.4999983909999983 0.5791131260000029

0.9491459730000003 0.5000017289999974 0.4208868739999971